Journal of Alloys and Compounds 509 (2011) 80–86

Contents lists available at ScienceDirect

Journal of Alloys and Compounds

journal homepage: www.elsevier.com/locate/jallcom

Ferromagnetism in ZnTe:Cr film grown on Si(1 0 0)

D. Soundararajan[a,f], P. Peranantham[a,c], D. Mangalaraj[a,b,*], D. Nataraj[a], L. Dorosinskii[d], J. Santoyo-Salazar[e], J.M. Ko[f,**]

[a] Thin Films and Nanomaterials Laboratory, Department of Physics, Bharathiar University, Coimbatore 641 046, India
[b] Department of Nanoscience and Technology, Bharathiar University, Coimbatore 641 046, India
[c] Laboratoire "EnVironnement et Minéralurgie" UMR 7569 CNRS, INPL-ENSG, B.P. 40, 54501 VandoeuVre-lés-Nancy, France
[d] National Institute of Metrology (TUBITAK-UME), P.K. 54, 41470 Gebze-Kocaeli, Turkey
[e] Centro de Investigación y de Estudios Avanzados de Instituto Politécnico Nacional, Departamento de Física, Av. IPN 2508, San Pedro Zacatenco, C.P. 07360, A.P. 14-740, 07000 México, D.F., Mexico
[f] Division of Applied Chemistry and Biotechnology, Hanbat National University, San 16-1, Dukmyung, Yusong, Daejon 305-719, South Korea

ARTICLE INFO

Article history:
Received 26 February 2009
Received in revised form 21 August 2010
Accepted 26 August 2010

Keywords:
ZnTe:Cr film
Magnetic domains
M–H curve
M–T measurements

ABSTRACT

$Zn_{1-x}Cr_xTe$ ($x = 0.0$ and 0.05) films were grown on Si(1 0 0) substrate by using thermal evaporation method. The structure of the films was investigated by X-ray diffraction and it showed the formation of ZnCrTe phase with an amorphous background, which indicated poor crystallinity. Composition analysis by XPS disclosed the presence of antiferromagnetic Cr_2O_3 and Cr precipitates. Magnetic domains were observed by using magnetic force microscopy at ambient temperature and the result showed anisotropic domains with an average size of 3.5 nm. Magnetic field dependence of magnetic moment measurements showed obvious hysteresis loop with a coercive field of 121 Oe at 300 K. Temperature dependence of magnetic moment showed short-range ferromagnetic order. The Curie temperature was estimated to be 354.5 K.

1. Introduction

Ferromagnetic dilute magnetic semiconductors (DMS) are getting attention and are important materials for the use in spin electronics devices. The primary issue for a material to act as source of spin current injection/magnetic storage layer is that it must be ferromagnetic well above room temperature and the prepared film must exhibit good crystallinity without any secondary phase [1–4]. Nowadays, a large number of attempts have been made to see ferromagnetic properties in different semiconductor hosts by doping with transition metal impurities. These attempts have been oriented to develop and understand the ferromagnetism at and above room temperature to realize a new class of spintronics devices [2,5].

So far, a lot of work has been done for the synthesis of novel DMS films with room temperature ferromagnetism based on III–V and II–VI compound semiconductors. Studies of transition metal (TM) doped II–VI compound semiconductors start to attract a lot of attention as TMs have lack of solubility in III–V compound semiconductors than in II–VI semiconductors [6,7]. Spin glass or antiferromagnetism was observed in II–VI compound semiconductors such as ZnTe when doped with Fe, Mn, Co [8]. However, highly p doped ZnTe films showed ferromagnetism at the temperature of 3 K when doped with Mn [9]. As an alternative way, when TM impurity such as Cr is doped into II–VI semiconductor hosts, ferromagnetic order was observed without any need of 'p' or 'n' type doping [10]. In this case, Cr played a dual role by providing 'p' type nature and as well as ferromagnetic behavior in the host semiconductor [11,4]. Saito et al. [11–13] and Ozaki et al. [14,15] have reported a linear relationship between T_c and Cr-doping concentration for ZnTe:Cr samples prepared by molecular beam epitaxy (MBE) system. They also found a T_c value slightly above 300 K for $x = 0.20$. A thorough literature survey shows that most of the investigation was done on ZnTe:Cr films grown on GaAs(1 0 0) substrate by MBE technique. Still large number of research groups is doing work on this material to understand further about its magnetic, electronic and optical properties. In this article, ZnTe:Cr films was prepared by using ther-

* Corresponding author at: Department of Nanoscience and Technology, Bharathiar University, Coimbatore 641 046, India.
Tel.: +91 0422 2425458; fax: +91 0422 2422387.
** Corresponding author. Tel.: +82 42 821 1545; fax: +82 42 821 1569.
E-mail addresses: dmraj800@yahoo.com (D. Mangalaraj), jmko@hanbat.ac.kr (J.M. Ko).

0925-8388/$ – see front matter © 2010 Elsevier B.V. All rights reserved.
doi:10.1016/j.jallcom.2010.08.103

mal evaporation method and its magnetic properties were done by using surface sensitive MFM and bulk sensitive SQUID magnetometry in order to understand about ferromagnetic nature of the sample.

2. Experimental details

2.1. Film deposition

Appropriate weights of high-purity Zn, Te and Cr (Alfa Aeser) metals were taken weighted together inside two separate quartz ampoules for the preparation of $Zn_{1-x}Cr_xTe$ alloys with $x = 0.0$ and 0.05. The ampoules were vacuum-sealed at a vacuum of 10^{-5} Torr and then they were kept inside a horizontal tube rotating furnace. In case of pure ZnTe, the ampoule was maintained at 600 °C for 12 h. In the case of ZnTe:Cr, the ampoule was maintained at 1100 °C for 24 h. In both cases, the temperature of the furnace was slowly increased step-by-step to the set value. After the reaction had been carried out for suitable time period, the temperature was slowly decreased in steps to room temperature. The molten alloy was taken out and made into fine powder by grinding in a mortar and then used for the growth of films. The $Zn_{1-x}Cr_xTe$ compound powder with $x = 0.0$ and 0.05 were thermally evaporated from a tungsten dimple source onto well-cleaned Si(1 0 0) substrates under a vacuum of 4×10^{-5} Torr at ambient temperature. The growth of each $Zn_{1-x}Cr_xTe$ film with $x = 0.0$ and 0.05 were performed individually.

2.2. Characterization

X-ray diffraction measurements were recorded in the 2θ scan range of 20–80° by using a X-ray diffractometer [Model – Shimadzu (XRD-6000), $\lambda = 1.5406$ Å]. XPS measurements were carried out using an Escalab 220iXL system (VG Scientific Inc.) with a monochromatic Mg Kα X-ray source (1284.6 eV). The ultimate XPS determination accuracy was of about 0.1 at.%. The relative atomic percentage of Zn, Te and Cr were obtained by using XPS peak fit software. Ex situ surface magnetic domain pattern of ZnTe:Cr film was performed at room temperature by using Scanning Probe Microscopy (SPM) (JEOL JSPM-4210). Topography of film was scanned by AFM in Tapping™ mode and magnetic domains were analyzed by lift mode, MFM. A magnetic cantilever tip NSC14/Co–Cr, Mikro-Masch, Co. was used with a resonant frequency of 160 kHz. The magnetic domains were observed with lift interaction in height of 25 nm and output of 0.025 A/V. The 2D and 3D images, profiles, and domains measurements were processed with the software win SPM DPS, JEOL Ltd. Magnetic data of the ZnTe:Cr film was collected using a commercial SQUID magnetometer (Quantum Design MPMS – XL Superconducting Magnet) both at liquid helium and room temperatures.

3. Results and discussion

3.1. Structural analysis

X-ray diffraction pattern of source materials ($Zn_{1-x}Cr_xTe$ alloys) with $x = 0.0$ and 0.05 in powder form were compared to ensure its crystalline quality as shown in Fig. 1(a) and (b). As can be seen, the diffraction peaks along (1 1 1), (2 0 0), (2 2 0), (3 1 1), (2 2 2) and (4 0 0) are observed to fit very well with the reported data for the bulk cubic ZnTe lattice and with JCPDS data [16]. It is evident that significant difference in the doped samples spectrum can be detected in comparison to the undoped ZnTe. In general, the shift of diffraction peak towards lower angle side is commonly observed for Cr doped ZnTe. It is therefore expected that significant change of the lattice parameter can be induced and the XRD spectra of the undoped and doped samples are not identical. This indicates that Cr is well incorporated into ZnTe system. This shows the formation of pure ZnCrTe/ZnTe cubic zinc-blende phase without any secondary phase.

The XRD of vacuum evaporated ZnTe and ZnTe:Cr films deposited on Si(1 0 0) in the 2θ scan range between 20° and 80° is shown in Fig. 2(a) and (b). Diffraction pattern of the ZnTe film shows a main peak along (1 1 1) reflection without any amorphous background indicating cubic zinc-blende structure as observed by Akram et al. for ZnTe film grown on glass by using vacuum evaporation method [17]. The diffraction pattern of ZnTe:Cr film shows a strong peak at 61.94° along (4 0 0) and a weak peak at 25.39° along (1 1 1) crystallographic directions indicate the presence of ZnCrTe cubic zinc-blende phase. The (4 0 0) peak is similar

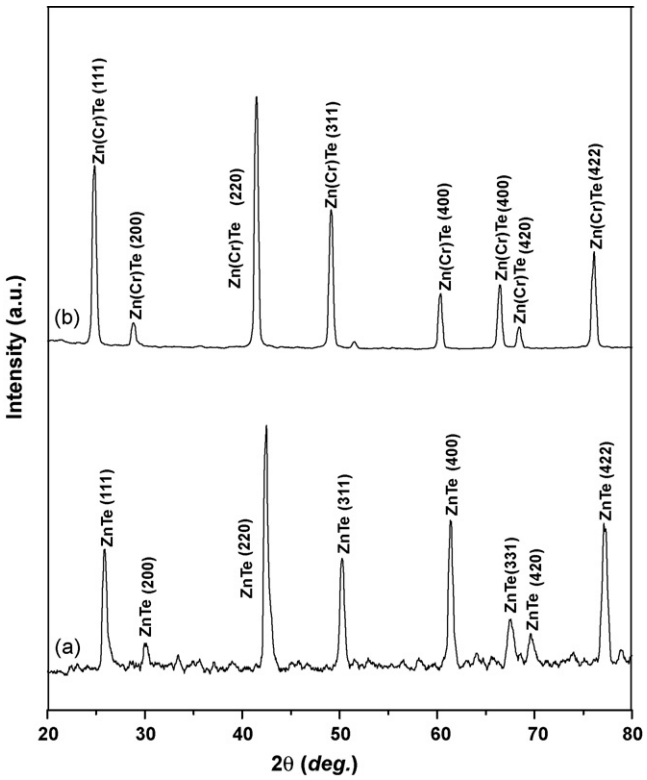

Fig. 1. X-ray diffraction patterns of (a) ZnTe and (b) ZnTe:Cr alloy powder samples.

to the results observed by Kuroda et al. [18,19] for ZnTe:Cr thin films grown on GaAs(1 0 0) by MBE technique. The lattice parameter along the growth direction was deduced from the diffraction angle of the (1 1 1) peak of ZnTe and ZnTe:Cr films. The calculated lattice parameter values of ZnTe and ZnTe:Cr films are 5.96 and 6.08 Å, respectively. The observed weak reflection along (1 1 1) direction and increment in lattice parameter is an indication that Cr has substitutionally incorporated into the ZnTe lattice. Besides, an amorphous background was noticed in the 2θ scan range of 21–48° along with the cubic ZnCrTe phase. This amorphous background is owing to the poor crystalline nature of the film. This indicates,

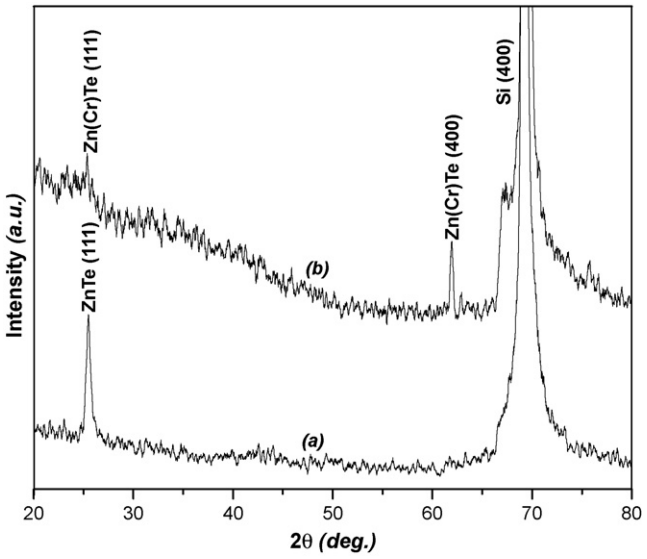

Fig. 2. X-ray diffraction patterns of vacuum evaporated (a) ZnTe and (b) ZnTe:Cr films grown on Si(1 0 0) substrate.

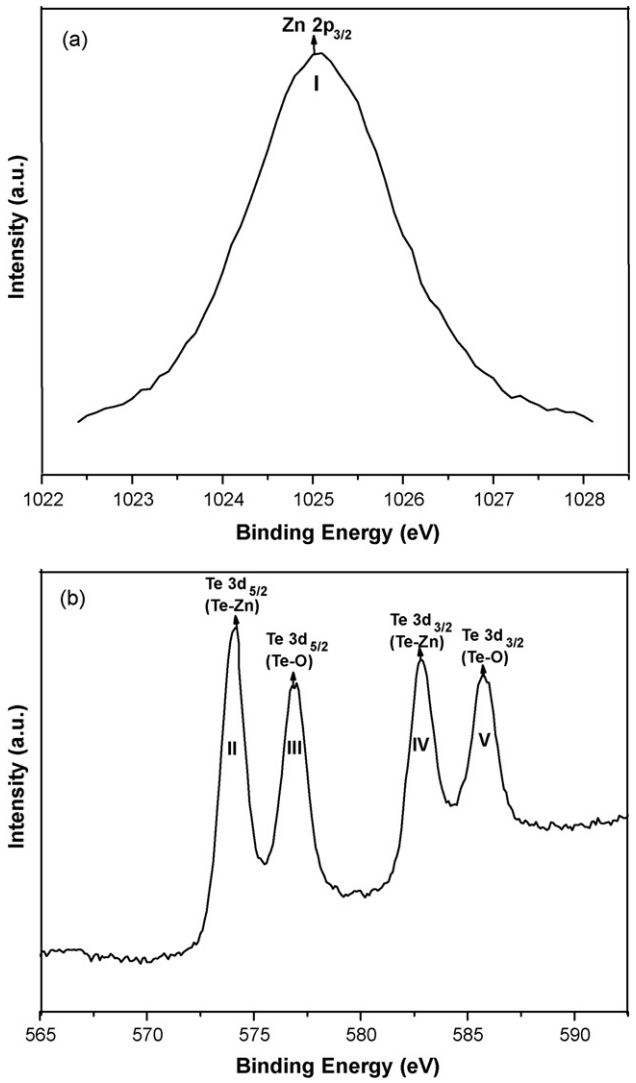

Fig. 3. (a and b) High resolution surface XPS spectra of ZnTe film.

the film consists amorphous ZnCrTe/CrTe in addition to ZnCrTe crystalline phase.

3.2. XPS analysis

The microscopic surface composition of the prepared ZnTe and ZnTe:Cr films were investigated by high resolution XPS. The obtained results are shown in Figs. 3(a), (b) and 4(a)–(e). The most probable assignments to the origin of components in ZnTe and ZnTe:Cr films are presented in Tables 1 and 2, respectively [20]. In the case of ZnTe, there appeared a single peak for Zn at 1025.08 eV and which correspond to $2p_{3/2}$ transition. In the case of Te, there appeared two peaks at 574.2 and 582.9 eV and which correspond to $3d_{5/2}$ and $3d_{3/2}$ transitions, respectively. In addition, in adjacent

Table 1
Assignments to the component of peaks of the high resolution surface XPS scans of the ZnTe film.

Component	Binding energy (eV)	Assignment
I (Zn $2p_{3/2}$)	1025.08	Zn–Te
II (Te $3d_{5/2}$)	574.2	Te–Zn
IV (Te $3d_{5/2}$)	576.9	Te–O_2
VI (Te $3d_{3/2}$)	582.9	Te–Zn
VIII (Te $3d_{3/2}$)	585.7	Te–O_2

Table 2
Assignments to the component of peaks of the high resolution surface XPS scans of ZnTe:Cr film.

Component	Binding energy (eV)	Assignment
I (Zn $2p_{3/2}$)	1021.8	Zn–Te
II (Te $3d_{5/2}$)	573	Te–Zn
III (Cr $2p_{3/2}$)	574	Cr–Te
IV (Cr $2p_{3/2}$)	573.7	Cr–Cr
V (Te $3d_{5/2}$)	576.5	Te–O_2
VI (Cr $2p_{3/2}$)	575.6	Cr_2–O_3
VII (Te $3d_{3/2}$)	583.3	Te–Zn
VIII (Cr $2p_{1/2}$)	583.5	Cr–Te
IX (Te $3d_{3/2}$)	586.5	Te–O_2
X (Cr $2p_{1/2}$)	586.6	Cr_2–O_3

to these two peaks there appeared another set of peaks at 576.9 and 585.7 eV, which are again correspond to $3d_{5/2}$ and $3d_{3/2}$ transitions but are due to the oxide phase of Te (Te–O). The spectra correspond to ZnTe:Cr film was deconvoluted since the core level binding energy of Cr and Te are close to each other. The presence of Cr^{2+} in ferromagnetic Zn(Cr)Te/(Cr)Te phase was noticed at its corresponding binding energy 574 eV [20,21]. In addition, the peak at 576 and 573.7 eV indicates the presence of Cr_2O_3 and Cr, respectively [21,22]. This shows the presence of secondary phases such as Cr and Cr_2O_3 which are antiferromagnetic in nature [23,24]. Since the Cr valence is identical in the ZnCrTe and CrTe phases, any ferromagnetic property should arise from the +2 state of chromium. Therefore, these two phases might be the origin of the observed ferromagnetic behavior. The stoichiometry of ZnTe and ZnTe:Cr films were determined by using 2p peak for Zn, 3d peaks for Te and 2p peaks for Cr. The estimated values of relative atomic percentage of Zn, Te and Cr are given in Table 3.

3.3. Magnetic properties

3.3.1. Magnetic domains

Magnetic force microscopy is becoming one of the most used techniques for the imaging of magnetic domains [25]. Prior to measurements, the film was exposed to minute argon gas flow and, subsequently, the topographic observation was carried out by AFM. Then the magnetic domains were observed in remnant state by using MFM. Topography and MFM images of ZnTe:Cr film is shown in Fig. 5(a) and (b). From the AFM image as in Fig. 5(a), the obtained average grain size value is 85 nm. MFM image shows the magnetic domains within the grains and the shape of domains is not uniform as in Fig. 5(b). This can be associated with the shape of particles, interactions between neighborhood and the magneto static forces in the grain boundary. Fig. 6 (a) shows magnetic domains of the marked region in Fig. 5(b). The marked region comprises a grain and grain boundary. The domains are strong in the interior of grain and weak in the grain boundary, suggesting the domains are anisotropic in the selected area. The domain interactions over the surface as shown in Fig. 6(a) was focused in the selected area of 20 nm × 20 nm for further analysis as illustrated in Fig. 6(b). The result clearly shows nanometric bubble shaped bright and dark zones signifying domains with opposite polarization. The distribution of domains in the profile (Fig. 6(c)) indicates that the average

Table 3
Relative atomic percentage of Zn, Te and Cr elements as evaluated from the high resolution surface XPS spectra of the ZnTe and ZnTe:Cr films.

Samples	Relative at.% of		
	Zn	Te	Cr
ZnTe	52.1	47.17	–
ZnTe:Cr	45.0	50.03	4.97

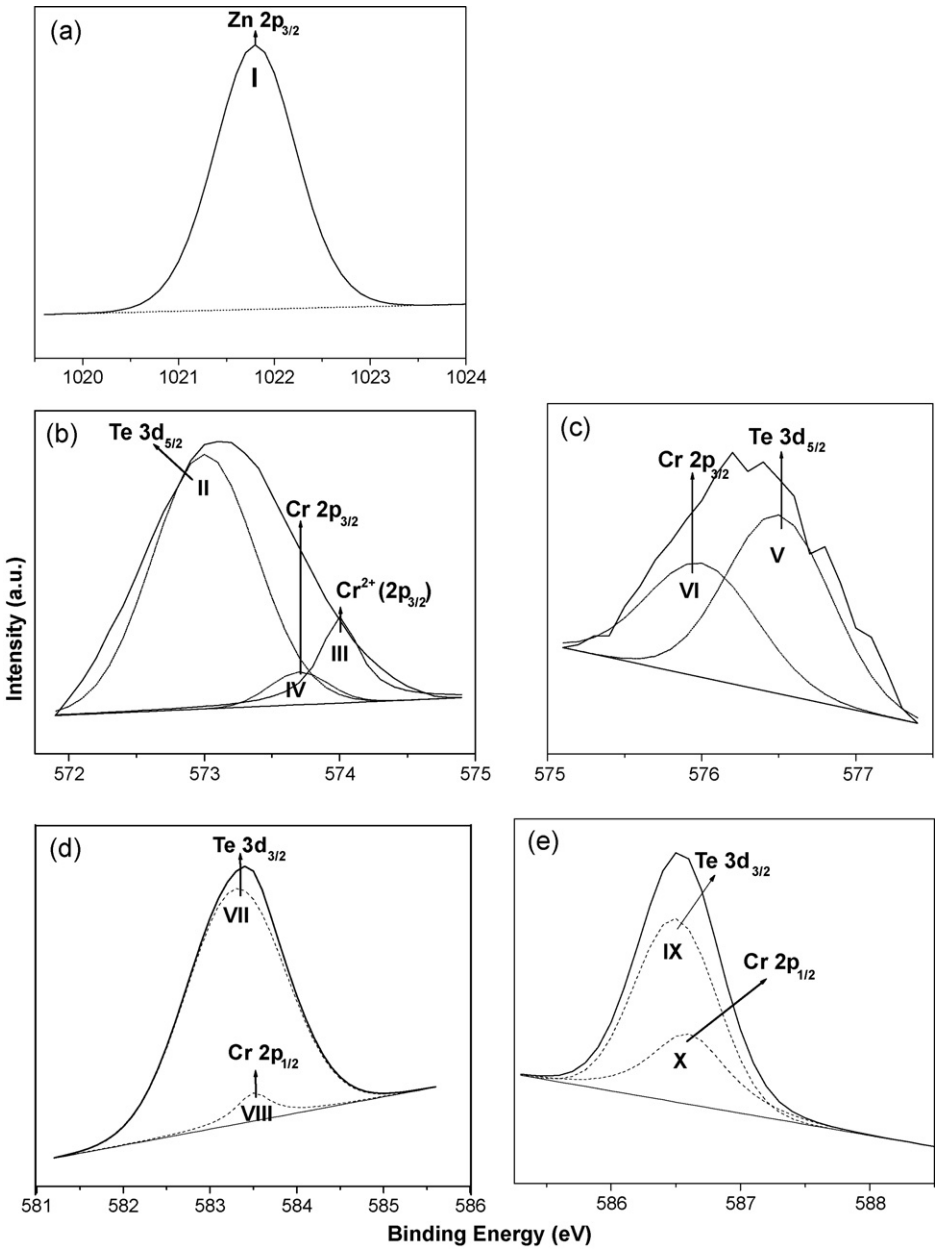

Fig. 4. (a–e) Deconvoluted high resolution surface XPS spectra of ZnTe:Cr film.

size of domains over the film surface is 3.5 nm and it supports an existence of magnetization at the surface of the film. The observed domains must have originated from the cubic ZnCrTe and from amorphous ZnCrTe/CrTe.

3.3.2. Magnetic moment measurements

Fig. 7 shows the plots of magnetic moment as a function of magnetic field for ZnTe:Cr film recorded at temperatures 10, 77 and 300 K. The results show hysteresis loops with coercive fields of 177, 133 and 121 Oe at temperatures 10, 77 and 300 K, respectively. It should be noted that the ferromagnetic feature remains even at $T = 300$ K. An attempt was made to use Arrott plot analysis of the obtained M–H data [26,4]. In this work, the Arrott plots of measured hysteresis loop at temperatures 10, 77 and 300 K are plotted and are shown in the inset of Fig. 7. The plot shows non-linearity at all the magnetic field range, which means that the mean field theory does not apply and the film has short-range interactions [27]. At the same time, the curvature did not go through the origin even when the temperature reaches 300 K. It points out that the saturation magnetic moment does not go to zero and it implies the persistence of minute ferromagnetic order even when the field is removed. It suggests the shorter range ferromagnetic order and it resulted in the small values of saturation magnetic moment and remnant magnetic moment as can be seen from the hysteresis curves.

It is also useful to analyze the magnetic moment as a function of temperature in order to determine the type of magnetic behavior of the film with respect to temperature. Two measurement procedures were used to obtain the behavior of magnetic moment versus temperature. The sample was first cooled in zero field from the room temperature to 10 K. Next the measurement field $(H_{\perp}) = 1000$ Oe was applied and the temperature was then increased and the zero-field-cooled (ZFC) curve was recorded. The temperature was next reduced without changing the measurement field and the field cooled (FC) curve was recorded. Fig. 8 exhibits the measurement of magnetic moment, with an applied magnetic field

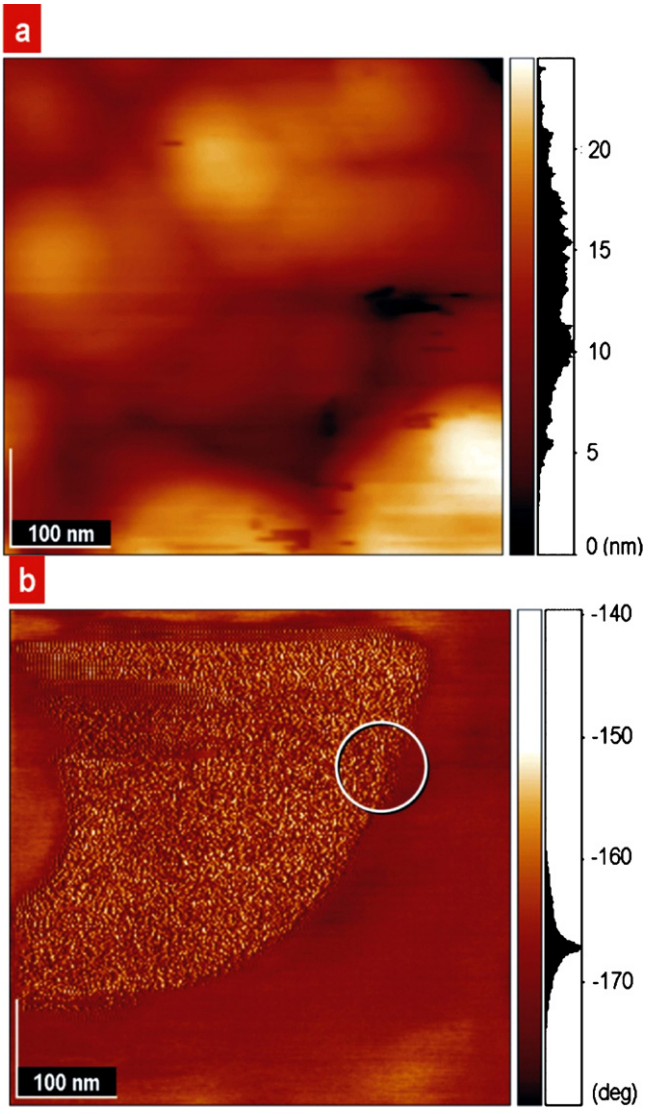

Fig. 5. 2D view of AFM and MFM images of ZnTe:Cr film. (a) Nanoparticles in the scanned area of 500 nm × 500 nm. (b) Distribution of anisotropic nanometric magnetic domains in the same area.

of ($H_{\perp}$) = 1000 Oe, as a function of temperature, both after cooling in zero field (ZFC) and while cooling in a field (FC). The results show irreversibility of ZFC and FC curves up to a temperature of 354.5 K. For the ZFC process, the magnetic moment of the film slightly increases thereafter decreases. This increase in magnetic moment clearly indicates a ferromagnetic like behavior of the prepared film. The wide hump and non-monotonic shape of the ZFC curve indicate that there is no typical first order magnetic phase transition from ferromagnetic to superparamagnetic behavior at 91 K (symbolized as T_{B1}). Supportingly, the M versus H measurements on the film yield an obvious hysteresis loop with a coercive field of 121 Oe and the remanent magnetic moment of 4.3×10^{-6} emu at 300 K. This indicates that no paramagnetic behavior can be expected prior to 300 K and hence a distribution in the blocking temperatures is expected. For the FC process, thermal fluctuations decrease upon decrease of temperature and spins prefer to align mostly in the direction of the applied magnetic field. The states of higher energy along the applied field direction become more populated. Consequently, the magnetic moment of the film increases with decrease of temperature and no blocking temperature (T_B) is observed since T_B must be lower than the applied temperature range. Moreover, the ZFC and FC curves are irreversible up to a temperature of 354.5 K (symbolized as T_{B2}). Magnetic phase transition from ferromagnetic to paramagnetic state can take place at and above 354.5 K where the ZFC and FC curves bifurcate. However, the broad maximum observed on the ZFC curve occurs at a lower temperature of 91 K (T_{B1}) than T_{B2}. Such a behavior generally signalizes certain particle size distribution in the prepared ZnTe:Cr film; while a fraction of the nanoparticles already freeze at T_{B1}, the majority fraction of the largest particles in the film is being blocked at T_{B2} resulting in a distribution of the blocking temperature (T_{B1}, T_{B2}) in the film [28,29]. These results indicate clearly a shorter range ferromagnetic behavior which persists up to a temperature of T_{B2} (354.5 K). Thereafter, the film behaves like paramagnetic. These results imply that the Curie temperature is slightly greater than 354.5 K and that there is a ferromagnetic behavior above room temperature. Since the prepared ZnTe:Cr film is poor crystalline nature, in addition to cubic zinc-blende ZnCrTe phase, the presence of amorphous ZnCrTe/CrTe also contribute to the observed high T_c.

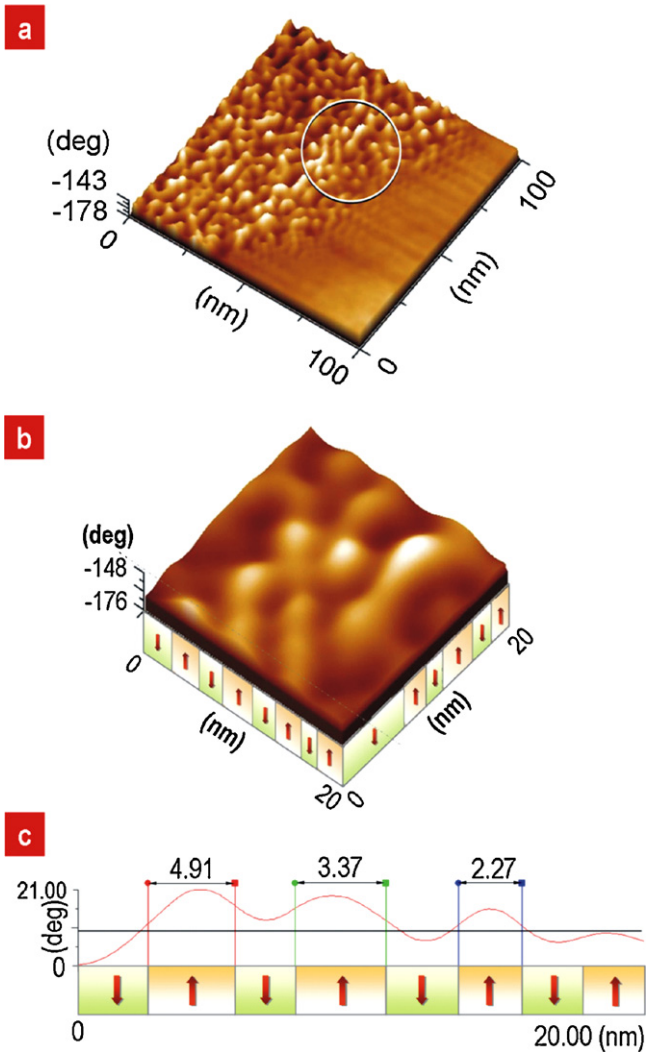

Fig. 6. High resolution magnetic domains in the selected region of Fig. 5(b). (a) 3D view of domains in the core and grain boundary in area of 100 nm × 100 nm (b) Domains in the selected area of 20 nm × 20 nm. The domains below of 3D image show bright zones which correspond to positive charge (↑) and dark zones indicates a negative charge (↓) and (c) Profile of domains in cross section of the image of (b). The average domain size over the film surface is 3.5 nm.

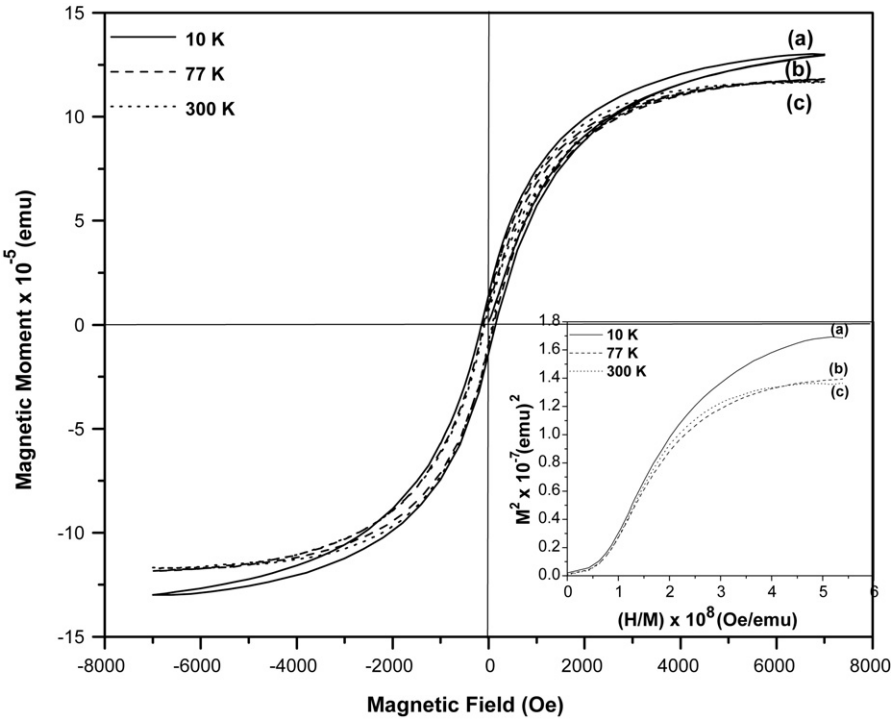

Fig. 7. Magnetic moment as a function of magnetic field plot of ZnTe:Cr film measured at temperatures (a) 10 K, (b) 77 K and (c) 300 K. Diamagnetic contribution from the Si substrate was subtracted. An obvious hysteresis loop is observed from the *M* versus *H* plot confirming a ferromagnetic ordering induced by the Cr doping in ZnTe. The inset shows the Arrott plots of magnetic moment data.

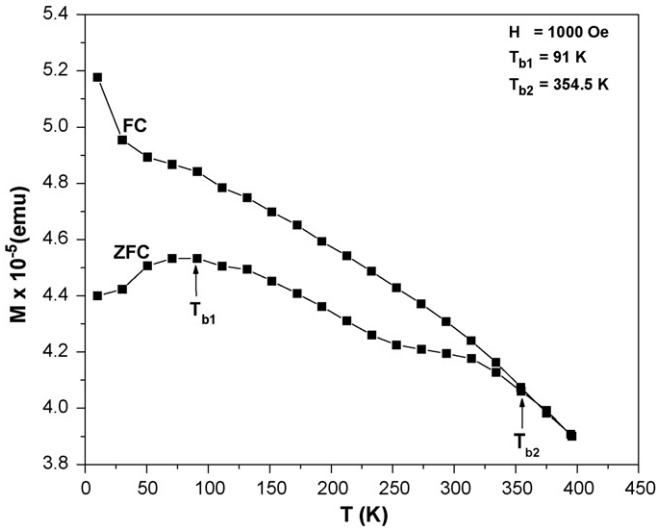

Fig. 8. Zero-field cooled (ZFC) and field-cooled (FC) magnetic moment measurements of ZnTe:Cr, at a magnetic field 1000 Oe applied perpendicular to the film plane.

4. Conclusion

$Zn_{1-x}Cr_xTe$ films with $x = 0.0$ and 0.05 were grown on Si(1 0 0) substrate by a simple thermal evaporation method. Structure of Cr doped ZnTe film showed the presence crystalline ZnCrTe phase as well as amorphous ZnCrTe/CrTe, which indicated poor crystallinity nature of the film. XPS analysis showed the presence of antiferromagnetic Cr_2O_3 and Cr precipitates. Ferromagnetic hysteresis loop and the remnant state nanometric domain structure were observed at room temperature. The magnetic moment versus temperature curves indicated a short-range ferromagnetic behavior, and the Curie temperature was estimated to be 354.5 K. The origin of the ferromagnetic behavior is expected not only from the crystalline ZnCrTe, but also from amorphous ZnCrTe/CrTe.

Acknowledgements

This work was partly supported by the World Class University Program (R33-2008-000-10147-0) from Ministry of Education, Science and Technology, Korea. We have a very special acknowledgement to C. Flores-Morales from Instituto de Investigaciones en Materiales, IIM-UNAM by his technical support in AFM characterization.

References

[1] S.H. Chun, S.J. Potashnik, K.C. Ku, P. Schiffer, N. Samarth, Phys. Rev. B 66 (2002) 100408 (R).
[2] W.G. Wang, C. Ni, T. Moriyama, J. Wan, E. Nowak, J.Q. Xiao, Appl. Phys. Lett. 88 (2006) 202501.
[3] I. Zutic, J. Fabian, S. Das Sarma, Rev. Mod. Phys. 76 (2004) 323.
[4] H. Saito, V. Zayets, S. Yamagata, K. Ando, Phys. Rev. Lett. 90 (2003) 207202.
[5] H. Saito, S. Yuasa, K. Ando, J. Appl. Phys. 97 (2005) 10D305.
[6] T. Dietl, H. Ohno, Science 287 (2000) 1019.
[7] S. Mackowski, et al., Appl. Phys. Lett. 83 (2003) 3575.
[8] J.K. Furdyna, J. Appl. Phys. 64 (1988) R29.
[9] D. Ferrand, et al., Physica B 1177 (2000) 284.
[10] J. Blinowski, P. Kacman, J.A. Majewski, Phys. Rev. B 53 (1996) 9524.
[11] H. Saito, V. Zayets, S. Yamagata, K. Ando, Phys. Rev. B 66 (2002) 081201.
[12] H. Saito, V. Zayets, S. Yamagata, K. Ando, J. Appl. Phys. 93 (2003) 6796.
[13] H. Saito, S. Yamagata, K. Ando, J. Appl. Phys. 95 (2004) 7175.
[14] N. Ozaki, N. Nishizawa, S. Kurodo, K. Takita, J. Phys.: Condens. Matter 16 (2004) s5773.
[15] N. Ozaki, N. Nishizawa, S. Marcet, S. Kuroda, K. Takita, J. Supercond. 18 (2005) 29.
[16] JCPDS, X-ray Powder Diffraction File, Joint Committee for Powder Diffraction Standards (Card Numbers: 80-0022 & 80-0009).
[17] K.S. Akram, Z. Ali, A. Maqsood, Appl. Surf. Sci. 143 (1999) 39.
[18] N. Ozaki, N. Nishzawa, S. Marcet, S. Kuroda, O. Eryu, K. Takita, Phys. Rev. Lett. 97 (2006) 037201.
[19] S. Kuroda, N. Ozaki, N. Nishizawa, T. Kumekawa, S. Marcet, K. Takita, Sci. Technol. Adv. Mater. 6 (2005) 558.

[20] C.D. Wagner, W.M. Riggs, L.E. Davis, J.F. Moulder, C.E. Muielenberg, Handbook of X-ray Photoelectron Spectroscopy, Physical Electronics Industries, Eden Prairie, MN, 1976.
[21] C. Xu, M. Hassel, H. Kuhlenbeck, H.J. Freund, Surf. Sci. 258 (1991) 23.
[22] X.-Y. Li, E. Akiyama, H. Habazaki, A. Kawashima, K. Asami, K. Hashimoto, Corros. Sci. 39 (1997) 1365.
[23] D. Soundararajan, D. Mangalaraj, D. Nataraj, L. Dorosinskii, J. Santoyo-Salazar, J. Phys.: Conf. Ser. 153 (2009) 012048.
[24] S.N. Mishra, S.K. Srivastava, J. Phys.: Condens. Matter 20 (2008) 285204.
[25] M.H. Ham, S. Yoon, Y. Park, J.M. Myoung, Appl. Surf. Sci. 252 (2006) 6289–6293.
[26] A. Arrott, Phys. Rev. 108 (1957) 1394.
[27] J.G. Bohnet, P.M. Shand, J. Goertzen, J.E. Shield, D. Schmitter, G. Shelburne, D.L. Leslie-Pelecky, Am. J. Und. Res. 6 (2007) 19–30.
[28] P.M. Shand, C.C. Stark, D. Williams, M.A. Morales, T.M. Pekarek, D.L. Leslie-Pelecky, J. Appl. Phys. 97 (2005) 10J505.
[29] J.P. Vejpravová, V. Sechovský, D. Nižňanský, J. Plocek, A. Hutlóv, J.-L. Rehspringer, WDS'05 Proceedings of Contributed Papers, Part III, 2005, pp. 518–523.